Princeton Plasma Physics Laboratory

PPPL- 4759

PPPL- 4759

Radial Resolution Enhancement of the NSTX Thomson Scattering Diagnostic

B.P. LeBlanc, A. Diallo, G. Labik, and D.R. Stevens

May, 2012

PPPL PRINCETON PLASMA PHYSICS LABORATORY

Prepared for the U.S. Department of Energy under Contract DE-AC02-09CH11466.

Princeton Plasma Physics Laboratory
Report Disclaimers

Full Legal Disclaimer

Trademark Disclaimer

PPPL Report Availability

Princeton Plasma Physics Laboratory:

http://www.pppl.gov/techreports.cfm

Office of Scientific and Technical Information (OSTI):

http://www.osti.gov/bridge

Related Links:

U.S. Department of Energy

Office of Scientific and Technical Information

Fusion Links

Radial resolution enhancement of the NTSX Thomson scattering diagnostic [a)]

B.P. LeBlanc,[1] A. Diallo,[1] G. Labik,[1] and D.R. Stevens,[1]

[1]*Princeton Plasma Physics Laboratory, Princeton, New Jersey 08543, USA*

(Presented XXXXX; received XXXXX; accepted XXXXX; published online XXXXX)
(Dates appearing here are provided by the Editorial Office)

Current magnetic confinement plasma physics research has increased the demand for radial resolution in profile diagnostics, in particular in the edge and pedestal regions. On NSTX, an upgrade of the existing multi-point Thomson scattering (MPTS) diagnostic has been implemented in order to respond to the research program needs. Twelve new radial channels have been added bringing the total number of positions to 42. Four previously un-instrumented fiber bundles were put in service. Eight existing "active" fiber bundles were divided in two sub-bundles in order to increase spatial resolution. Twelve radial channels now cover the pedestal region with a resolution near one centimeter, which is comparable to the thermal-ion Larmor radius of high power plasmas. Fifteen radial channels cover the core and internal transport barrier regions. Two additional channels were added, one near the inner edge and one in the outer scrape-off layer, which now has five radial channels. The intersection of the focused viewing optics field of view with a finite-width laser beam results in major-radius crosstalk between adjacent fiber sub-bundles. A discussion and calculation of the crosstalk will be presented. This work is supported by U.S. Dept. of Energy Contract Nos. DE-AC02-09CH11466.

I. INTRODUCTION

The Multi-Point Thomson Scattering (MPTS) diagnostic system has been providing time dependent T_e and n_e profile measurements on NSTX for ten years[1]. A phased implementation continues, made possible by the original installation of key components. For example the mirror viewing optics has been fully populated with 36 fiber-optics bundles. Bundle subsets were progressively instrumented as resources became available. Similarly, two of three installed cradles support 30-Hz Nd:YAG lasers. Since 2005, MPTS has been operating with these two lasers, 60-Hz being the routine timing arrangement, and 30 major radius channels stemming from the instrumentation of twenty-nine fiber bundles. The collecting optics views 93% of the machine aperture at the midplane, which includes both sides of the magnetic axis and the outer scrape off layer (SOL). In this paper, we review the implementation of twelve addition radial channels resulting in a total of 42. In response to NSTX's research needs, the radial array was densified primarily at the outer edge transport barrier (ETB) region and new channels were added to the internal transport barrier (ITB) region. Furthermore two extra channels were added: one near the top in the inner ETB and one more in the SOL. A specially designed fiber-optics holder (FOH) supports the fiber-bundle array at the focus of the mirror optics viewing along the laser beam path. Spacers between adjacent bundles provide mechanical strength and prevent major-radius viewing overlap. The overlap can result from the intersection of the field of view depth and the finite size laser beam. Thomson scattering optical arrangements, where the laser beam and collection optics are on the midplane, are susceptible to major radius overlap. The effect is exacerbated when the beam path is not purely radial as is the case for the MPTS.

II. INITIAL FIBER OPTICS SPLITTING

The MPTS design provides the option of dividing the output end of a fiber bundle into different branches for increased spatial resolution. In 2005, we tested the idea and "coherently" divided the output end of a fiber bundle into two sub-bundles viewing adjacent sections of the original bundle viewing span. The two branches were assigned to different polychromators. The original 19-fiber bundle was viewing at major radius, R, of 144 cm. Figure 1 shows before and after division photographs obtained through back illumination. The conjoint bundles have respectively 10 and 9 fibers and view radial spans centered respectively at R= 144.5 and 143.6 cm. Subsequent TS measurements during plasma operation revealed that the modification was successful, the two conjoint channels providing meaningful measurements, well tested during the subsequent NSTX experimental campaigns. Figure 2 shows radial overlays at six consecutive times of T_e and n_e profiles during the H-mode phase of an NSTX NBI plasma. These partial spatial profiles include the ETB and the conjoint radial locations, indicated with a dashed line. Although the etendue is reduced by factor two, the size of the error bars remains acceptable. This could be attributed

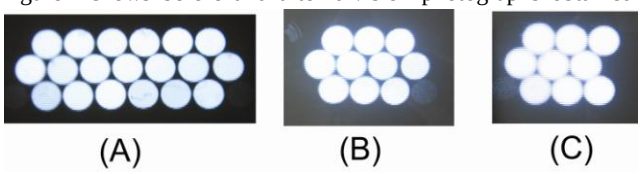

FIG. 1. Fiber bundle splitting, (A) original bundle; (B) 10-fiber sub-bundle; (C) 9-fiber sub-bundle

[a)]Contributed paper published as part of the Proceedings of the 19th Topical Conference on High-Temperature Plasma Diagnostics, Monterey, California, May, 2012.
[b)]Author to whom correspondence should be addressed: leblanc@pppl.gov

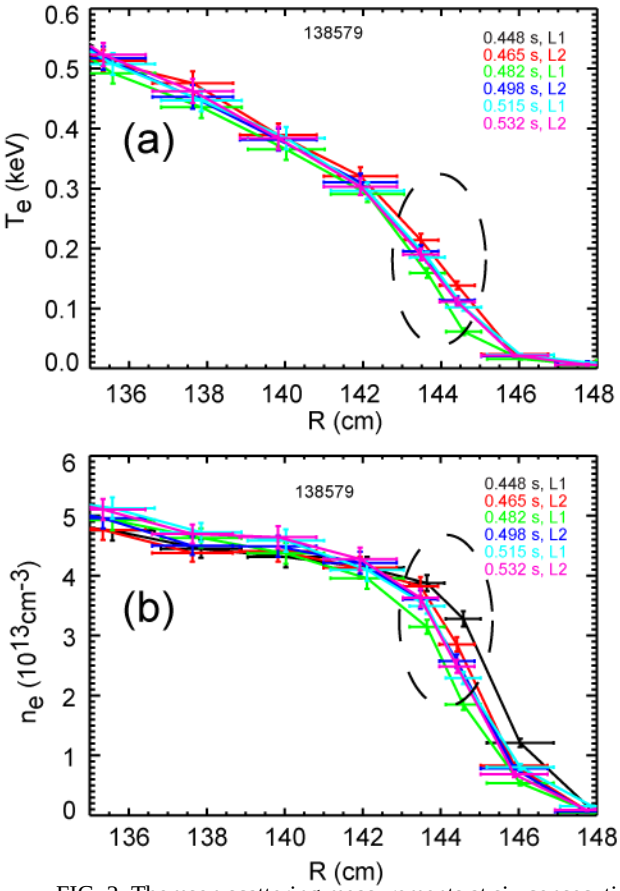

FIG. 2. Thomson scattering measurements at six consecutive times: T_e right panel and n_e on right panel. The conjoint radial locations are circled with a dashed line.

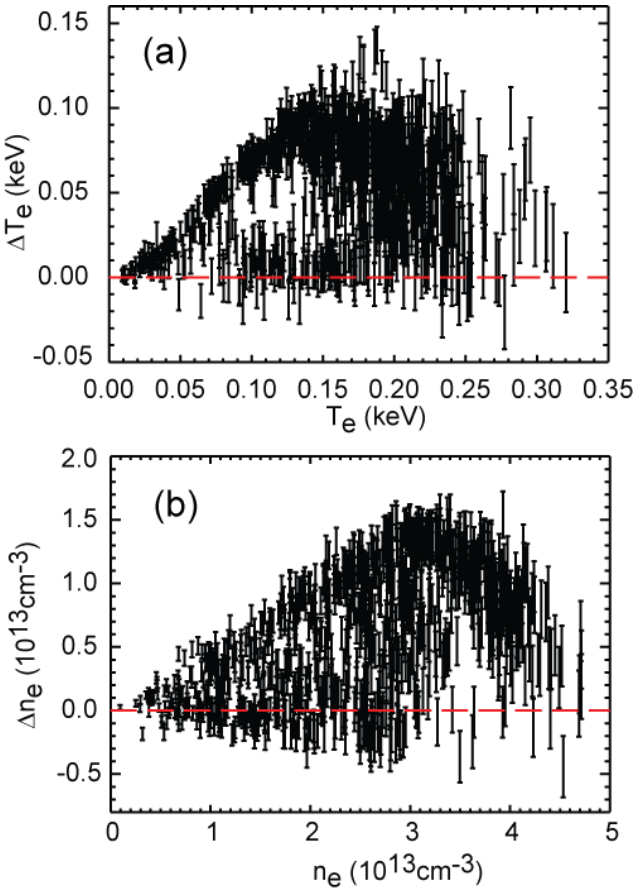

FIG. 3. Measurement difference in T_e and n_e between conjoint channels: (a) ΔT_e ; (b) Δn_e . Data shown against T_e or n_e at R=143.6cm.

to the fact that the collecting optics was overfilling the polychromator originally for larger values of R as is the case here. We also show a horizontal radial span bar for each position. The latter is computed based on geometric arguments and corresponds to the full measurement span. In Fig.3, we show plots of the difference between the inner and outer conjoint radial channels for a set of 961 measurements obtained during 21 discharges similar to one shown in Fig.2. Figure 3(a) shows ΔT_e = T_e(R=143.6cm) – T_e(R=144.5cm) and is displayed with its associated error $\delta\Delta T_e$ computed quadratically. Similarly in Fig3.(b), we see Δn_e and its error. From their definitions, both ΔT_e and Δn_e should normally be zero or positive since the conjoint channels cover the ETB. Indeed, one can see in both panels that ΔT_e and Δn_e range from zero to positive values. The measured ΔT_e and Δn_e are outside of the error bars indicating a low level of radial crosstalk. In fact the conjoint channels have been validated over thousands of plasma discharges and have provided routinely meaningful "research grade" data since their installation.

III. RADIAL RESOLUTION ENHANCEMENT

Based on the success of the "original" fiber bundle division, it was decided to continue using this technique in order to improve spatial resolution in response the research program needs. Eight additional fiber bundles were split in two. Furthermore four unused fiber bundles were instrumented. This implementation adds 12 new radial channels for a total of 42 spatial positions. We can see in Fig.4 an overlay of the center to center distance between adjacent radial channels for 30-channel and the 42

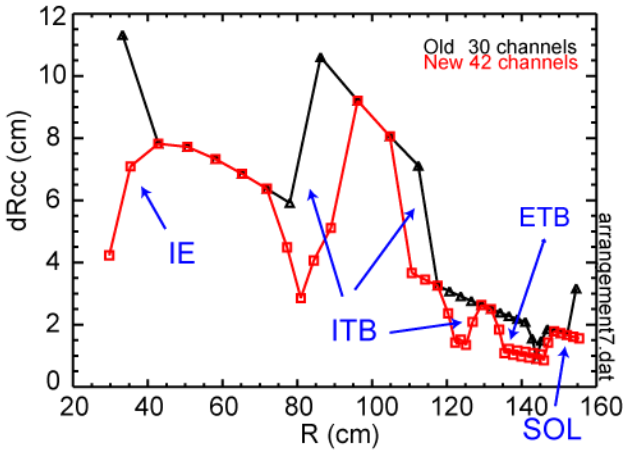

FIG. 4. Spatial position center to center distances for 30-channel and 42-channel configurations

channel arrangements. In the latter case, thirty-three fiber bundles are utilized: 24 full bundles and 9 divided into 18 sub-bundles. Special attention was given to the ETB, which now has six consecutive split fiber bundles. The spatial resolution of the ITB has also been improved. Finally two new channels were added: one at the inner ETB and one more to the SOL.

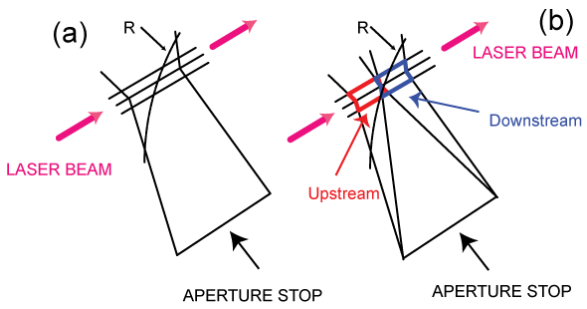

FIG. 5. Schematic illustration of major radius overlap: (a) fiber bundle before division; (b) conjoint sub-bundles after division. Drawing is not to scale.

Because no spacer separates the conjoint channel pairs, an estimate of radial overlap in the measurement needs being done. In the past MPTS has been supplying profile results with one-sigma "vertical" error bars for T_e, n_e and electron pressure p_e. But it also supplied an estimate of the major radial span over which the measurement occurs. The latter is based on one-dimensional estimates of the laser scattering length for each radial position and the corresponding values of the major radius. As for the first conjoint radial pair mentioned above, the radial span of each sub-bundle has been given a long lived temporarily approximation of half of the full bundle radial span. In the following we proceed to improved calculations in preparation for 42-channel MPTS operation on NSTX-U[2]. One can see in Fig.5 the geometry corresponding to fiber bundle division. The view is looking down at the midplan intersection of the viewing optics ray traces and the laser beam. The direction of the laser beam propagation is indicated by a magenta arrow. The full bundle geometry is seen in panel (a) and that of a divided bundle is seen in panel (b). An irregular hexagon marks the perimeter of the laser-and-optics intersection for each sub-bundle. In Fig.6, we show a scaled drawing of the geometry for the innermost fiber bundle that was divided. The nominal major radius is R≈80cm. We use the letters "u" and "d" to identify parameters corresponding to points which are respectively upstream and downstream of the laser beam propagation. We also chose the color red for upstream and blue for downstream. One can see sectors corresponding to circles of different major radius values. The sectors appear as straight lines on this scale, which are not at right angles with the laser direction, consistent with the MPTS geometry. The calculations can be divided in two parts: (1) using the geometrical extrema of the hexagons mentioned above; (2) distributing an even set of points within each of the hexagon and calculating average and standard deviation. Going back to the first calculation: one can compute the average major radius, *Ru*, of the upstream bundles as the average of the largest and smallest major radii found among the hexagon vertices. The major radial deviation can be defined as the difference between the two extrema just mentioned. If R_{hex} is the set of major radii corresponding to the six vertices of the upstream hexagon, then

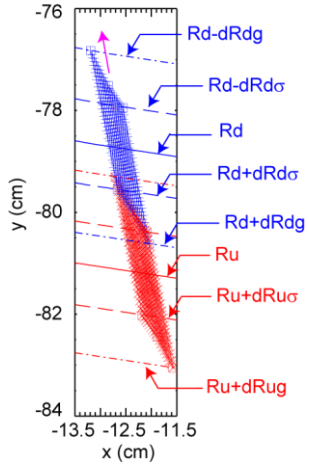

FIG. 6. Geometry for innermost fiber division. Nominal R ≈ 80cm.

we can write a geometrically defined upstream major radius as $Rug = \frac{Max(R_{hex})+Min(R_{hex})}{2}$ and its span as $ug = \frac{Max(R_{hex})-Min(R_{hex})}{2}$. A similar definition can be made for the downstream geometrically derived parameters *Rdg* and *dRdg*. In a second computation, Ndist=400 points are evenly distributed within each of the upstream and downstream hexagons. We compute the corresponding set of major radii R_{dist}. These points can be seen in Fig.6. Then one can compute the average $Ru\sigma = \frac{\sum R_{dist}}{N_{dist}}$ and the standard deviation $dRu\sigma = \sqrt{\frac{1}{N_{dist}-1}\sum(R_{dist} - Ru\sigma)^2}$. The calculations $Rd\sigma$ and $dRd\sigma$ follow in a straightforward manner for the downstream section. The calculations of *Rug* and Ruσ give essentially the same results: within less than 1 mm over most of the radial profile. For this reason, we simply use *Ru* and *Rd* in Fig. 6. Hence we see sectors with respective radius *Ru* and *Rd* corresponding to the upstream and downstream major radii. Also shown in the figure are sectors with radii *Rd±dRdg* corresponding to the extremum edges of the downstream geometry. Similar sectors are also drawn for the upstream geometry, although not all sectors are labeled to help visibility. We also show upstream and downstream sectors with radii Ru±dRuσ and Rd±dRdσ. These correspond to one-sigma standard deviation among the distributed points discussed above. The one-sigma radial span values is about half on the geometrical extrema calculation. While we intend to continue providing the MPTS profile data with its current "dR" based on the one-dimensional laser scattering length, we are considering adding the one-sigma evaluation as well, since it would be a better match to the one-sigma "vertical" error bars provided for T_e, n_e and p_e profiles. The radial overlap, expressed as a fraction of a sub-bundle radial

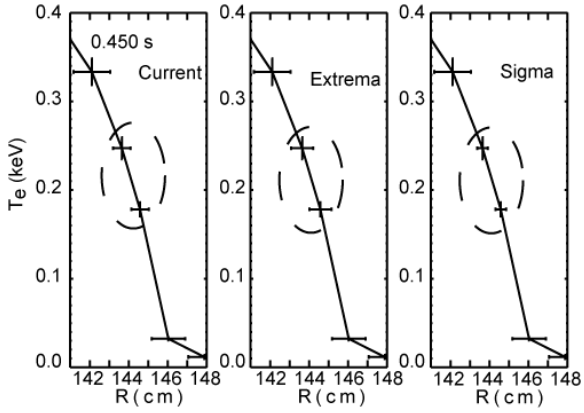

FIG. 7. Comparison of radial span evaluation: current, extrema and distribution (sigma)

span, varies from 0.24 to 0.34 when based on extrema calculations; it is nonexistent based on the one-sigma radial span. We can see in Fig.7 a side-by-side comparison of the three radial span calculations: current, extrema and distribution (Sigma). The calculation used currently falls between the extrema and one-sigma evaluation. This work is supported by U.S. Dept. of Energy Contract Nos. DE-AC02-09CH11466.

[1] B. P. LeBlanc, Rev. Sci. Instrum. 74, 1659 (2003) and refs therein

[2] A. Diallo, B. P. LeBlanc, G. Labik and D. Stevens at this conference, submitted to RSI

The Princeton Plasma Physics Laboratory is operated
by Princeton University under contract
with the U.S. Department of Energy.

Information Services
Princeton Plasma Physics Laboratory
P.O. Box 451
Princeton, NJ 08543

Phone: 609-243-2245
Fax: 609-243-2751
e-mail: pppl_info@pppl.gov
Internet Address: http://www.pppl.gov